

Supporting Information for

**Efficient Water Oxidation with Electromodified Langmuir-Blodgett Films of Pro-catalytic
[Co^{III}(N₂O₃)] Metallosurfactants on Electrodes**

Sunalee Gonawala, Habib Baydoun, Lanka Wickramasinghe, and Cláudio N. Verani*

Department of Chemistry, Wayne State University, Detroit, MI 48202, USA

Contentents

1. Experimental Section
 - a. Materials and Methods
2. Turnover Number, Faradaic Efficiency, and Onset Overpotential Calculations
3. Synthesis and Characterizations
4. Mass Spectrum for the Complex [Co^{III}(L^{N2O3})H₂O]
 - a. **Figure S1:** Experimental (bars) and simulated (line) isotopic distribution for the molecular ions of [Co^{III}(L^{N2O3})H₂O]
5. Electronic Spectrum for the Complex [Co^{III}(L^{N2O3})H₂O]
 - a. **Figure S2:** UV-visible spectrum of [Co^{III}(L^{N2O3})H₂O] in 1.0 x 10⁻⁵ dichloromethane solution
6. Electrochemical Data for the Complex [Co^{III}(L^{N2O3})H₂O]
 - a. **Figure S3:** Cyclic voltammogram of [Co^{III}(L^{N2O3})H₂O] in dichloromethane. Conditions: 0.1 M TBAPF₆ as supporting electrolyte; Glassy carbon (working), Pt wire (counter) and Ag/AgCl (reference); Scan rate: 100 mV s⁻¹
7. Langmuir-Blodgett Film Formation and Characterizations
 - a. **Figure S4:** AFM images of monolayer films deposited on mica substrates at different surface pressures with 5 μm scan size
 - b. **Figure S5:** IRRAS spectrum of C—H stretching region in comparison with KBr in bulk infrared spectra
8. Catalytic Studies
 - a. **Figure S6:** (a) Plot of current density vs. time before rinsing. (b) Plot of current density vs. time after rinsing.
 - b. **Figure S7:** Correlation between number of layers and final current density of the bulk electrolysis performed using the rinsed electrodes
 - c. **Figure S8:** SEM images obtained for (a) bare FTO electrode (b) LB 3 layers deposited FTO electrode before catalysis (c) LB 3 layers deposited FTO electrode after 12 h catalysis

- d. **Figure S9:** XPS scan of the Co 2p region for 11-layer FTO electrode
- e. **Figure S10:** IRRAS spectra of C—H stretching of 50-layer deposited film on FTO substrate region before catalysis and after catalysis after rinsing with organic solvents
- f. **Figure S11:** UV-visible data on 50-layer deposited electrodes before and after electrolysis.
- g. **Figure S12:** Charge passed through a 9-layer FTO electrode over 12 h electrolysis

1. Experimental Section

Materials and Methods

Reagents were used without further purification as purchased from commercial sources. $^1\text{H-NMR}$ spectra were recorded on a Varian 400 MHz instrument. Elemental analysis was measured by Midwest Microlab, Indianapolis, Indiana, using an Exeter CE440 CHN analyzer. ESI mass spectra were measured on a ZQ-Waters/Micromass high resolution mass spectrometer. The FT-IR spectra were obtained as KBr pellets from 4000 to 600 cm^{-1} using 64 scans on a Tensor 27 FTIR-spectrophotometer. UV-visible spectra were obtained using a SHIMADZU UV-3600 spectrophotometer. Electrochemical experiments were performed using a BAS 50W voltametric analyzer and bulk electrolysis was performed using a CHI600E voltametric analyzer. A standard three-electrode cell system was used for electrochemical experiments with glassy carbon as the working electrode, Pt coil (13 cm) as the auxiliary electrode, and an Ag/AgCl reference electrode filled with 1 M KCl under an argon atmosphere and at room temperature. Tetrabutylammonium hexafluorophosphate (TBAPF_6) was used as the supporting electrolyte and ferrocene was added to the solution as an internal redox standard. Redox potential values were recorded with reference to the experimental Fc/Fc^+ value.¹ A film was used for bulk electrolysis as deposited onto fluorine-doped tin oxide (FTO) glass plates with *ca.* 0.6 cm^2 surface area and used as the working electrode. All the voltamograms were recorded at a scan rate of 100 mV s^{-1} .

2. Turnover Number, Faradaic Efficiency, and Onset Overpotential Calculations

Turnover Numbers (TON) and Faradaic Efficiencies (%FE) were calculated using a procedure adapted from the literature.² A Gow-Mac 400 gas chromatograph (GC) was used for O_2 detection as equipped with a thermal conductivity detector and a 8 ft x 1/8 in 5 Å molecular sieve column operating at a temperature of 60 °C. Helium was the carrier gas at a flow rate of 30 mL/min. The GC was used to quantify the O_2 in the head space of the cell using atmospheric N_2 as internal standard. The concentration of dissolved O_2 was taken into account according to Henry's law.³ An example of such calculations is shown below.

	% O ₂	% N ₂	Ratio
Air	20.3	79.7	r _{air} = 0.2547
Blank	22.0	70.0	r _{blank} = 0.2821
LB	29.2	70.8	r _{LB} = 0.4124

Head space volume = 9.5 mL

Volume of solution = 36 mL

Henry's law constant = $769.23 \frac{\text{L}\cdot\text{atm}}{\text{mol}}$

n_{O_2} in head space before catalysis (A) = 82.5 μmol for 9.5 mL

O₂ produced in headspace = $\frac{r_{lb} - r_{blank}}{r_{air}} \times A = \frac{0.4124 - 0.2821}{0.2547} = 42.22 \mu\text{mol}$

O₂ dissolved = n_{O_2} final – n_{O_2} initial

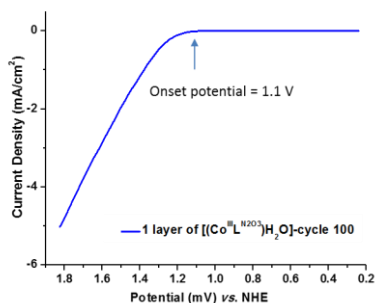
$$= \frac{p_{\text{O}_2 \text{ final}}}{K} * V_{\text{solution}} - \frac{p_{\text{O}_2 \text{ initial}}}{K} * V_{\text{solution}}$$

$$= (0.292 - 0.203) \left(\frac{36000 \mu\text{L}}{769.23 \left(\frac{\text{L}\cdot\text{atm}}{\text{mol}} \right)} \right) = 4.164 \mu\text{mol}$$

Total amount of O₂ produced = n_{O_2} in headspace + n_{O_2} dissolved = 4.164 + 42.22 = 46.384 μmol

n_{O_2} based on charge = $\frac{Q_{LB} - Q_{blank}}{4 \times 0.096485} = \frac{22.524 - 4.2144}{4 \times 0.096485} = 47.44 \mu\text{mol}$

Faradaic efficiency = $\frac{n_{\text{O}_2 \text{ experimental}}}{n_{\text{O}_2 \text{ charge}}} \times 100 = \frac{46.384}{47.44} \times 100 = 98 \%$



Onset overpotential is calculated as follows:

Onset overpotential = onset potential – thermodynamic potential

Onset potential = 1.1 V

Thermodynamic potential = $E^0 - 0.059\text{pH} = 1.23 - 0.64 = 0.6 \text{ V}$

Therefore the onset overpotential = 1.1 V – 0.6 V = 0.5 V

3. Synthesis and Characterizations

a. Synthesis of $[\text{Co}^{\text{III}}(\text{L}^{\text{N2O3}})\text{H}_2\text{O}]$

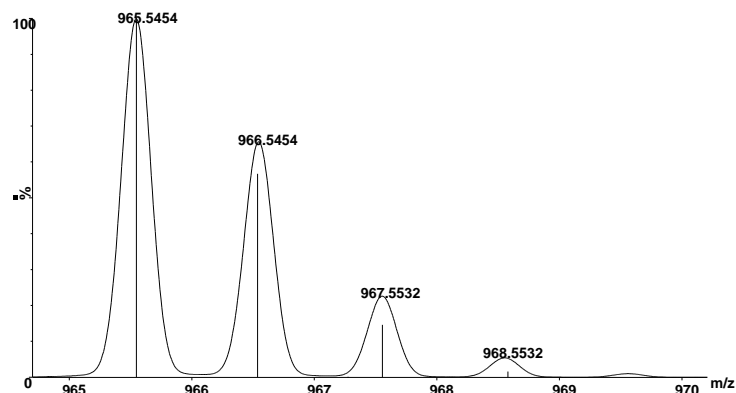
A 1:3 methanol:dichloromethane solution of $[\text{H}_2\text{L}^{\text{N2O3}}]$ (1 equiv.) and anhydrous NaOCH_3 (3 equiv.) was treated with a methanolic solution of $[\text{Co}^{\text{II}}(\text{H}_2\text{O})_6](\text{ClO}_4)_2$ (1 equiv.). The resulting solution was kept under mild reflux for 2 h after which a reddish brown precipitate was obtained via the slow evaporation of the parent solution. Yield: 85 % ESI (m/z^+) in CH_3OH = 965.5454 (100%) for $[\text{C}_{57}\text{H}_{81}\text{N}_2\text{O}_7\text{Co}+\text{H}^+]$ Anal. Calc. for $[\text{C}_{57}\text{H}_{83}\text{CoN}_2\text{O}_8 \cdot 2\text{H}_2\text{O}]$: C, 67.17; H, 8.60; N, 2.75% Found: C, 67.01; H, 8.48; N, 3.05% IR (KBr, cm^{-1}) 2869-2954 ($\nu_{\text{C-H}}$), 1613 ($\nu_{\text{C=C}}$, aromatic) 1592 ($\nu_{\text{C=N}}$), 1510 ($\nu_{\text{C=C}}$, aromatic), 1256 ($\nu_{\text{C-O-C}}$), 1128 ($\nu_{\text{C-O-C}}$).

b. Synthesis of $[\text{Ga}^{\text{III}}\text{L}^{\text{N2O3}}]$

The following used anhydrous solvents and manipulations were performed using air-free techniques. A solution of $[\text{H}_2\text{L}^{\text{N2O3}}]$ (0.30 g, 0.33 mmol) and anhydrous NaOCH_3 (0.06 g, 0.99 mmol) in methanol (15 mL) and dichloromethane (5 mL) was treated with a methanolic solution of GaCl_3 (0.08 g, 0.33 mmol). The resulting solution was heated at 50°C for 30 min, and was allowed to cool down to room temperature while under stirring for additional 90 minutes. The solvent was then removed under vacuum and the crude was dissolved in dichloromethane (20 mL) and filtered through celite. Finally, the solvent was removed under reduced pressure to yield a yellow precipitate. This precipitate is the amine species that gets converted to its imine counterpart during deposition.⁴ Yield: 72 % ESI (m/z^+) in CH_3OH = 977.5532 for $[\text{C}_{57}\text{H}_{83}\text{N}_2\text{O}_7\text{Ga}+\text{H}^+]$ Anal. Calc. for $[\text{C}_{57}\text{H}_{83}\text{GaN}_2\text{O}_7 \cdot 2\text{H}_2\text{O}]$: C, 67.51; H, 8.65; N, 2.75% Found: C, 67.19; H, 8.33; N, 2.84% IR (KBr, cm^{-1}) 3189 ($\nu_{\text{N-H}}$), 2869-2954 ($\nu_{\text{C-H}}$), 1607 ($\nu_{\text{C=C}}$, aromatic), 1514 ($\nu_{\text{C=C}}$, aromatic), 1270 ($\nu_{\text{C-O-C}}$), 1131 ($\nu_{\text{C-O-C}}$).

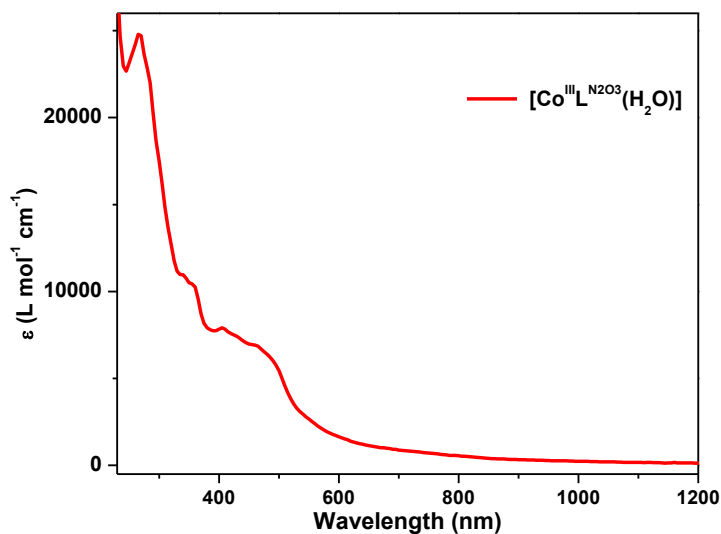
4. Mass Spectrum for the Complex $[\text{Co}^{\text{III}}(\text{L}^{\text{N2O3}})\text{H}_2\text{O}]$

Figure S1: Experimental (bars) and simulated (line) isotopic distribution for the molecular ions of $[\text{Co}^{\text{III}}(\text{L}^{\text{N2O3}}) + \text{H}^+]^+$



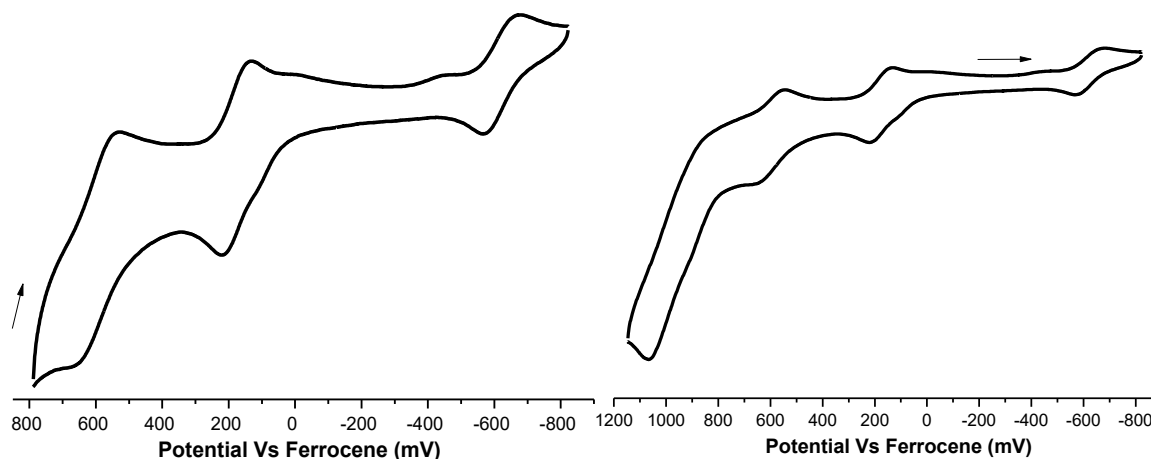
5. Electronic Spectrum for the Complex $[\text{Co}^{\text{III}}(\text{L}^{\text{N2O3}})\text{H}_2\text{O}]$

Figure S2: UV-visible spectrum of $[\text{Co}^{\text{III}}(\text{L}^{\text{N2O3}})\text{H}_2\text{O}]$ in 1.0×10^{-5} dichloromethane solution



6. Electrochemical Data for the Complex $[\text{Co}^{\text{III}}(\text{L}^{\text{N2O3}})\text{H}_2\text{O}]$

Figure S3: Cyclic voltammograms of $[\text{Co}^{\text{III}}(\text{L}^{\text{N2O3}})\text{H}_2\text{O}]$ in dichloromethane. Conditions: 0.1 M TBAPF₆ as supporting electrolyte; glassy carbon (working), Pt wire (counter), Ag/AgCl (reference). Scan rate: 100 mV s^{-1} .



7. Langmuir-Blodgett Film Formation and Characterizations

The compression isotherm for the cobalt- $[\text{N}_2\text{O}_3]$ complex was measured using an automated KSV 2000 minitrough at 23°C with a 10 mm/min compression rate. Barnstead NANOpure water with $18.2 \text{ M}\Omega \text{ cm}^{-1}$ resistivity was used as the subphase. A $50 \mu\text{l}$ aliquote of a 1.0 mg/ml chloroform solution of the complex was spread on the subphase and allowed to equilibrate for 20 min before compression.

Figure S4: AFM images of monolayer films deposited on mica substrates at different surface pressures with 5 μm scan size.

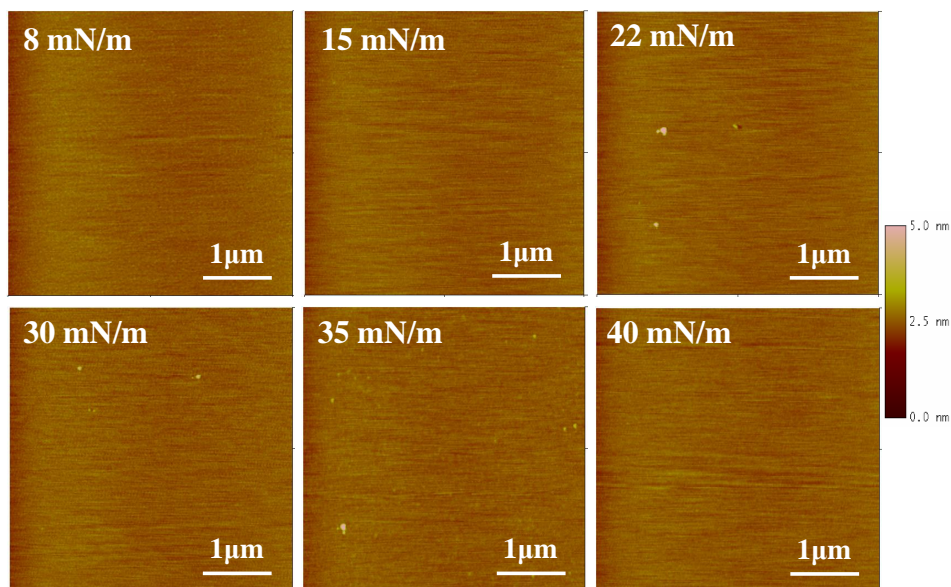
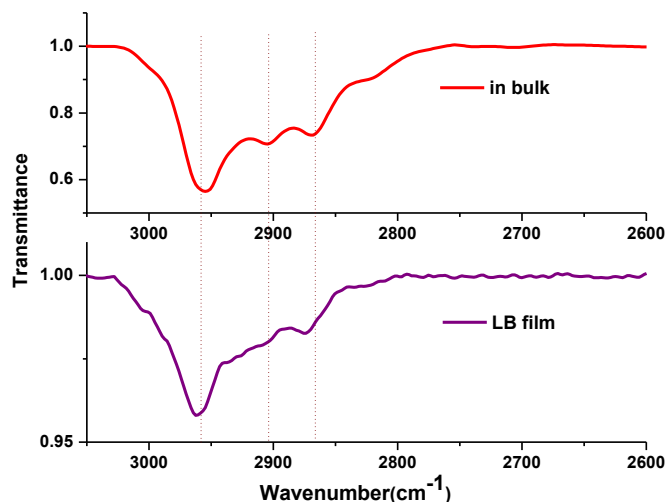


Figure S5: IRRAS spectra of the C-H stretching region in comparison with KBr in bulk infrared spectra.



8. Catalytic Studies

The catalytic experiments were carried out using a CHI600E voltammetric analyzer. Several FTO electrodes coated with 1 to 13 layers of $[\text{Co}^{\text{III}}(\text{L}^{\text{N}2\text{O}3})\text{H}_2\text{O}]$ were used with an area of *ca.* 0.6 cm^2 , a 12-inch Pt coil was used as the auxiliary electrode, and an Ag/AgCl electrode filled with 1 M KCl was used as reference. Bulk electrolysis was performed in a custom-made airtight H-type cell. The working and reference electrodes were placed in the same compartment and

the Pt-coil auxiliary electrode was placed in another compartment separated by a fine frit. Both the compartments were filled with 0.1 M sodium borate buffer to assure a constant pH 11. The working electrode was subjected to 1 h electrolysis under an applied potential of 1.2 V. The amount of oxygen was determined using a Gow-Mac 400 gas chromatograph equipped with a thermal conductivity detector using atmospheric nitrogen gas as internal standard (examples of calculations have been included in Section 2). Error bars represent the standard deviation of at least three different experiments.

Figure S6: (a) Plot of current density vs. time before rinsing; (b) Plot of current density vs. time after rinsing.

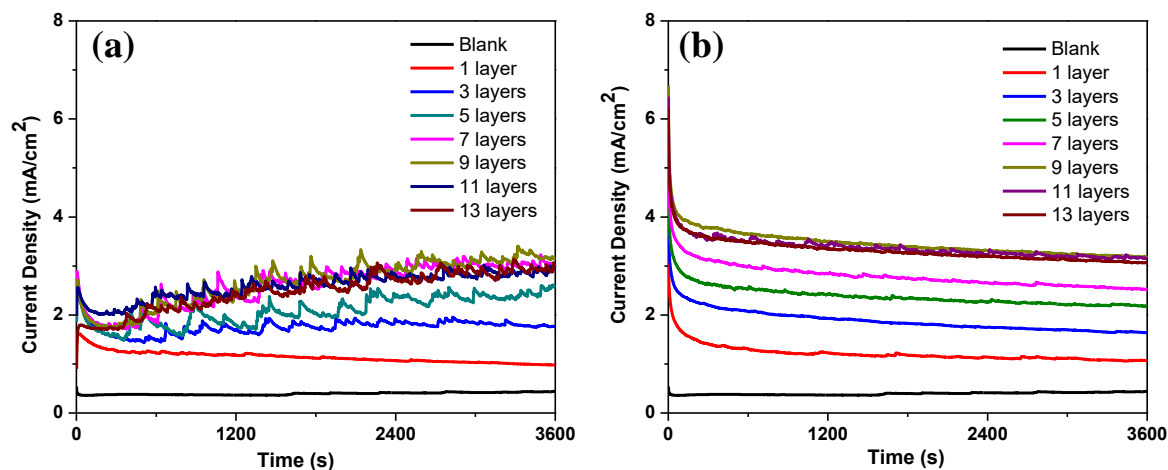


Figure S7: Correlation between number of layers and final current density of the bulk electrolysis performed using the rinsed electrodes.

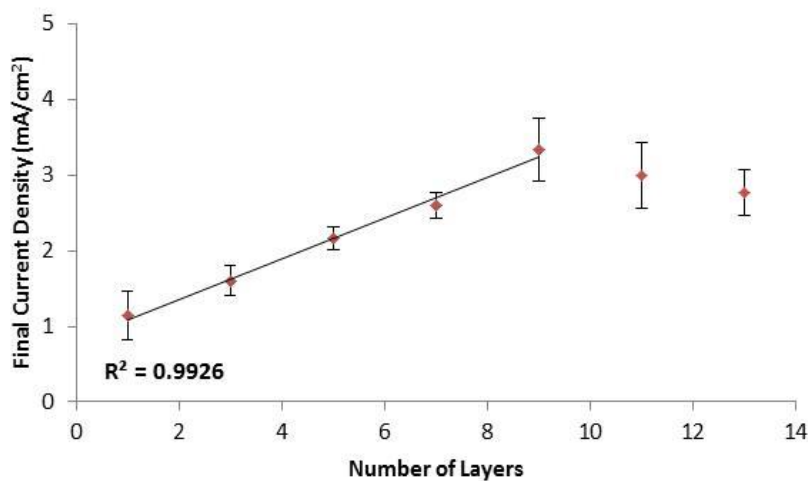


Figure S8: SEM images obtained for (a) bare FTO electrode, (b) 9-layer LB film deposited onto an FTO electrode after 12 h catalysis.

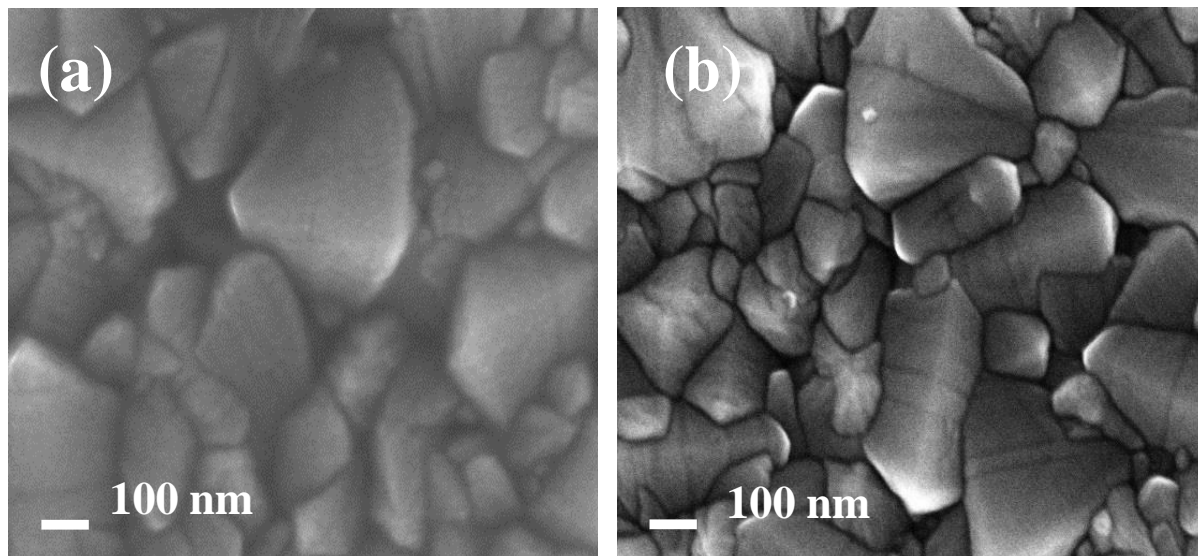


Figure S9: XPS scan of the Co 2p region for 11-layer FTO electrode.

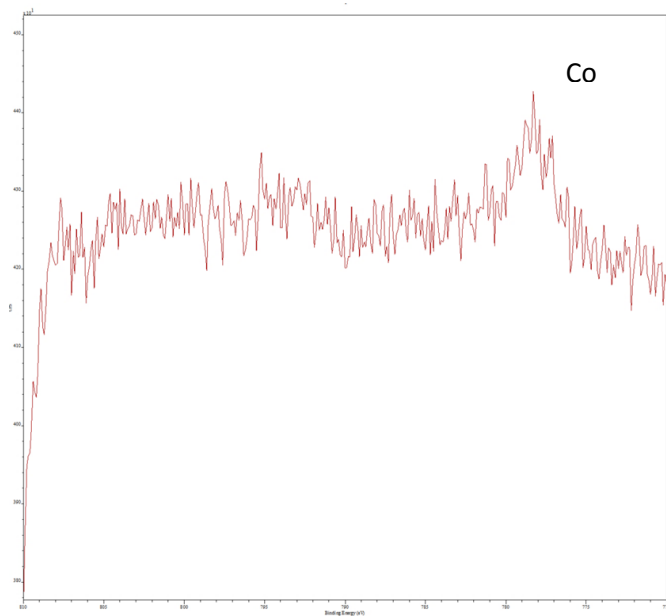


Figure S10: IRRAS spectra of C—H stretching of 50-layer deposited film on FTO substrate region before catalysis and after catalysis after rinsing with organic solvents.

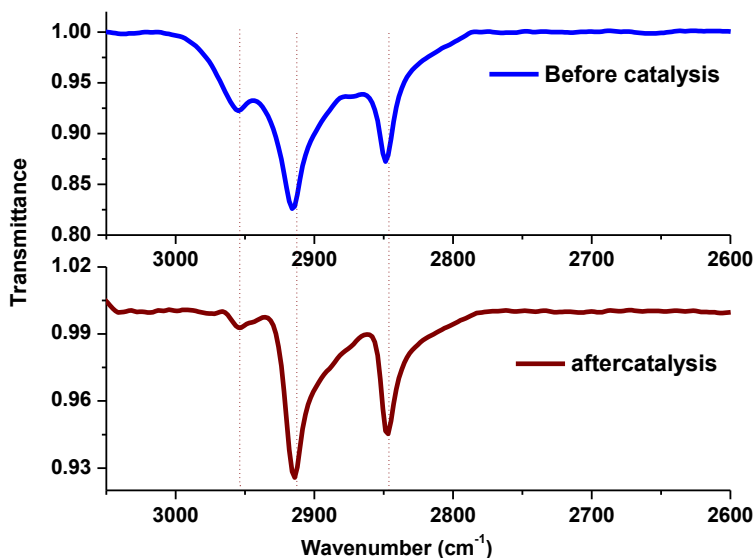


Figure S11: UV-visible data on 50-layer deposited electrodes before and after electrolysis.

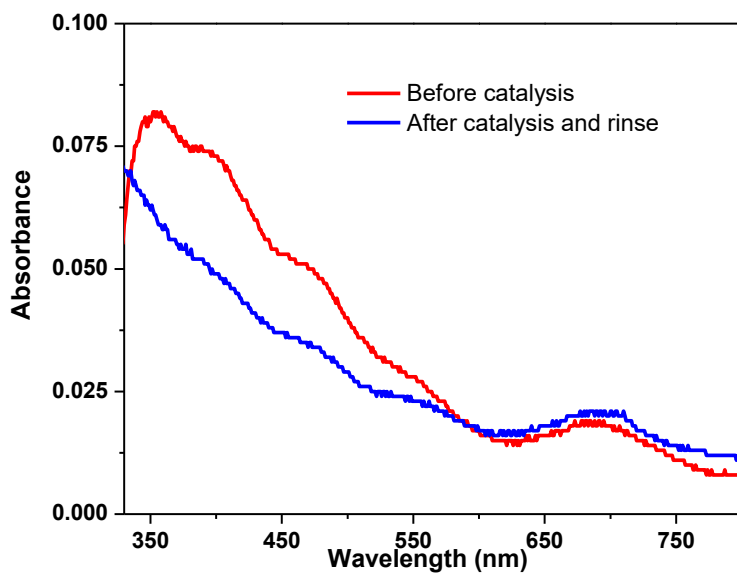
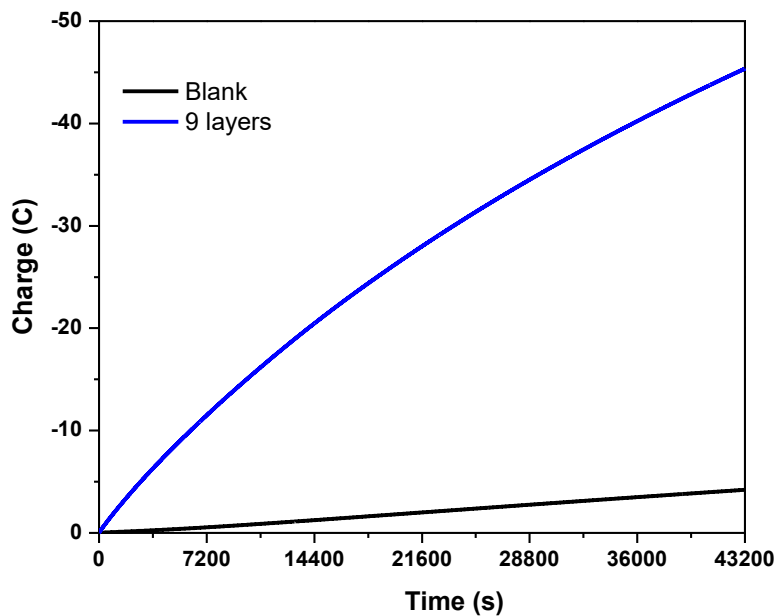


Figure S12: Charge passed through a 9-layer FTO electrode over 12 hours of electrolysis.



1. R. Gagne, C. Koval, and G. Licenski, *Inorg. Chem.*, 1980, **19**, 2854.
2. W. Lee, S. B. Mucoz, D. A. Dickie, and J. M. Smith, *Angew. Chem. Int. Ed.* 2014, **53**, 9856.
3. R. Sander, *Atmos. Chem. Phys.* 2015, **15**, 4399.
4. L. D. Wickramasinghe, M. M. Perera, L. Li, G. Mao, Z. Zhou, and C. N. Verani, *Angew. Chem. Int. Ed.* 2013, **52**, 13346; *Angew. Chem.* 2013, **125**, 13588.